Computational and Theoretical Chemistry 1229 (2023) 114337

Contents lists available at ScienceDirect

Computational and Theoretical Chemistry

journal homepage: www.elsevier.com/locate/comptc

Understanding the mechanism of thermal decomposition of benzoylformic acid

Daniel F. Giraldo-Alzate [a,*], Daniela Becerra [a], Silvia Quijano [b], Pablo Ruiz [a,c], Jairo Quijano [a], Jair Gaviria [a]

[a] *Laboratorio de Fisicoquímica Orgánica, Facultad de Ciencias, Universidad Nacional de Colombia, Medellín 050034, Colombia*
[b] *Programa de Microbiología, Facultad de Ciencias Básicas, Universidad Santiago de Cali, Cali, Colombia*
[c] *Facultad de Ciencias Exactas y Aplicadas, Instituto Tecnológico Metropolitano, Medellín, Colombia*

ARTICLE INFO

Keywords:
α-keto acids
Benzoylformic acid
Decarbonylation
Decarboxylation
PBE functional

ABSTRACT

In this work, the thermal decomposition of benzoylformic acid was studied computationally, including the decarboxylation reaction by two different mechanisms and an additional one for the decarbonylation of the compound. The PBE functional and 6-311+G(d,p) basis set in the gas phase and the aqueous solution were used. Transition states were modeled, kinetic and thermodynamic parameters were calculated for each reaction, and bonds evolution were tracked along the reaction coordinate by analysis of Wiberg bond indices. Two-step decarboxylation mechanism, initially proposed for the decomposition of pyruvic acid was found to be a probable mechanism for benzoylformic acid in gas phase, compared to the one-step decarboxylation and decarbonylation reaction.

1. Introduction

Benzoylformic acid is an intermediate compound to produce drugs [1]. Under the right conditions it is used as a reagent in obtaining oximes [2] and α-keto amides [3]. The compound is also a photoinitiator for the photochemical activation of molecules such as tetrahydrofuran (THF) [4]. Chemically it can be obtained by dehydrogenation, hydrolysis, acylation, or oxidation reactions on appropriate molecules [5–9]. Its production has also been reported from benzoyl cyanide using biocatalysts [1].

The thermolysis of benzoylformic acid and other α-keto acids has been conducted experimentally by other researchers [10–13] to elucidate the reaction mechanism. The products reported in the highest proportion are carbon dioxide, benzaldehyde, carbon monoxide and benzoic acid. Other experimental reports indicate that systems composed of dicarbonyl acids can be decomposed by ultraviolet irradiation processes [11,14–16]. Taylor, 1991 [12], studied the mechanism of thermal elimination of benzoylformic acid to produce carbon dioxide and benzaldehyde. The reaction was reported to be unimolecular and first order and take place through a four-center transition state, with a negative partial charge on the α-carbonyl group of the transition state. The author concluded that benzoylformic acid is more reactive than pyruvic acid, but less reactive than oxalic acid in the thermal elimination reaction. The author also indicates that benzoylformic acid in addition to the decarboxylation reaction can also thermally decompose by decarbonylation processes to produce carbon monoxide and the acid derivative, however, he considers the latter reaction to be less important to the conditions of the experiment.

The thermolysis reaction of α-keto-acids has also been studied theoretically. Chen L, et al, 1995 [17] reported the study of a series of these compounds at a low computational level, using semi-empirical methods (AM1), to verify the effect of the substituent group on the thermal processes of decarboxylation and decarbonylation. The authors discussed the activation energies and the characteristics of the transition states involved. They obtained values for the energy barriers of 375.37 and 276.98 $kJ.mol^{-1}$ for the one-step decarboxylation and decarbonylation of benzoylformic acid, respectively.

Saito K, et al, 1994 [13] in view of the difference in the parameters obtained in previous studies investigated experimentally using the shock waves method and computationally at HF/3-21G the unimolecular decomposition of pyruvic acid over the temperature range 850–1000 K. The researchers detected a product that could be hydroxyethylidene. They suggested a two-step mechanism, in the first-step the formation of the intermediate hydroxyethylidene occurs, which subsequently

---

[*] Corresponding author.
E-mail address: dafgiraldoal@unal.edu.co (D.F. Giraldo-Alzate).

https://doi.org/10.1016/j.comptc.2023.114337
Received 30 June 2023; Received in revised form 29 August 2023; Accepted 20 September 2023

isomerizes to acetaldehyde or vinyl alcohol. The kinetic data obtained agree with the Arrhenius parameters obtained by Taylor [12] and explain the ratio [acetaldehyde]/[CO_2] less than 1.

More recent computational studies on the thermal decomposition of pyruvic acid and oxalic acid have been published. Higgins, et al, 1997 [18] theoretically studied the thermal decomposition of oxalic acid in the range 400–430 K. Four reaction channels were proposed based on previous studies. Channel 1 leads the formation of a carbene intermediate, channel 2 involves direct decarboxylation of the reactant to formic acid, channel 3 occurs through a five-membered transition state to produce CO_2, CO, and H_2O. The proposed channel 4 studies the bimolecular reaction between a molecule of the carbene intermediate obtained from channel 1 with a molecule of oxalic acid, to generate formic acid. Their results indicate that the formation of dihydroxycarbene intermediate in the first-stage, and the subsequent bimolecular reaction with oxalic acid or water is the lowest energy route, therefore this is considered a feasible process for thermal decomposition.

Khavani et al, 2017 [19] also studied the thermal decomposition of oxalic acid with M06-L, M05-2X, B3LYP and X3LYP functionals, in the gas phase and in different solvents. They studied the first three reaction channels investigated by Higgins and two additional ones. Only two decomposition routes studied allow formic acid to be obtained and the most kinetically favorable of them is the one that involves the formation of the carbene intermediate.

Barquilla and Mayes, 2021 [20] studied the decomposition of pyruvic acid with the B2PLYP-D3BJ functional using the aug-cc-pVTZ basis set. From their results it was obtained that the direct route to form acetaldehyde and CO_2 requires 72.3 kcal.mol^{-1}, while the formation of the carbene-CO_2 complex requires 40.13 kcal.mol^{-1}.

The investigation of Taylor [12] on the decomposition of benzoylformic acid proposes a direct mechanism for decarboxylation to obtain benzaldehyde and CO_2, as well as a mechanism for decarbonylation through a five-membered transition state to produce benzoic acid and CO.

In the present work, the thermal decomposition reaction of benzoylformic acid at various temperatures, in the gas phase and in the aqueous solution has been studied computationally. The two reaction channels proposed by Taylor [12] were modeled. An additionally a two-stage decarboxylation mechanism was modeled with a carbene intermediate as was proposed for the decomposition of pyruvic and oxalic acids. These three reaction channels were studied to obtain kinetic and thermodynamic evidence that allows elucidating a feasible reaction mechanism for the decomposition of benzoylformic acid. It is also intended to analyze the structures and the reaction in terms of bond indices. To our knowledge, there is only one previous computational study of the thermal decomposition of benzoylformic acid performed at a low level [17].

The main purpose of this work is to address some questions and issues, such as: (1) Which of the studied mechanisms is the most suitable in accordance with the experimental values and is substantiated by the thermodynamic and kinetic outcomes? (2) How does the solvent effect influence the reaction mechanisms according to the method studied? (3) What observations can be made regarding the synchronicity of the studied mechanisms? These analyses will provide a more comprehensive understanding of the reaction mechanism involved in the thermal decomposition process of benzoylformic acid.

2. Material and methods

All structures representing each of the molecules involved in the reactions studied were fully optimized in the Gaussian 09 computational package [21]. Initial calculations were conducted with the M06-2X [22], PBE [23], B3LYP [24] functionals, and the Moller Pleset MP2 perturbation method [25]. 6–311+G(d,p) basis sets were used [26]. These density functionals were chosen because they are readily available in the Gaussian software and have been previously utilized within the research group in other studies. Furthermore, some of these were suggested by journal editors and referees, with consistently positive outcomes. The M06-2X functional is recommended for thermochemistry applications [22]. The PBE is a non-empirical popular functional that has reasonable accuracy over a wide range of systems [19,23,27]. The B3LYP functional is one of the most used in DFT calculations and has been used in the study of thermal decomposition of similar acids as oxalic acid [24,27]. The Moller Pleset MP2 is a basic electron correlation method that remains practically effective and relies on wave functions [25,27].

The geometrical parameters for all reactants, transition states and products of the studied reactions were optimized at the density functionals theory level (DFT) with the generalized gradient functional PBE-GGA [23] at 6–311+G(d,p). Vibrational frequency calculations were also performed to obtain the kinetic and thermodynamic parameters for each reaction investigated. Each structure was characterized as a minimum or a saddle point within the potential energy surface. The thermodynamic parameters were evaluated at 1.0 atm and five different temperatures in the range of 542.7–583.6 K. These values are based on experimental kinetics performed by Taylor [12]. It is a temperature range considered relatively high in which the decarbonylation reaction is somewhat inhibited and thermal decomposition occurs in a reasonable time.

Values for enthalpy and entropy were obtained according to the equations of standard thermodynamics [28]. The reactions were modeled in the gas phase and calculations in aqueous solution were conducted using the polarizable continuum model, making use of the integral equation formalism (IEFPCM) [29]. Within the polarizable continuous methods, the IEFPCM formalism is considered a robust method that adequately balances the charge effects with computational efficiency [30]. Each of the localized transition state structures was put through an intrinsic reaction coordinate (IRC) calculation [31] to verify that they connect to the corresponding minimum stationary points of reactants and products. The kinetic parameters were evaluated according to the classical transition state theory using the Eyring-Polanyi equations [32,33].

The molecular partitioning technique, natural bond orbital (NBO) [34,35] was applied using the NBO program [36] implemented in the Gaussian 09 computational package. Wiberg bond indices (β_i) [37] were obtained, which are interpreted as a measure of the order and strength of bonds within molecules. Additional indicators were calculated to follow the progress of the reaction in terms of bond breaking and bond formation, transition states (TS) and reactions were characterized in terms of average relative variation and absolute synchronicity (according to Eqs. (1)–(4)).

$\%EV = \delta\beta_i \times 100$(1) Percentage of evolution.

$\delta\beta_i = (\beta_i^{TS} - \beta_i^{R})/(\beta_i^{P} - \beta_i^{R})$(2) Relative variation. Represents advancement of the formation or breaking of a specific chemical bond within the transition state (TS) concerning the overall progression of it in relation to the elementary step.

$\delta\beta_{av} = 1/n\sum\delta\beta_i$(3) Average relative variation, n is the number of bonds to be considered in the reaction, that is, all those bonds that in the TS are in processes of rupture and formation. It represents an average of the relative variation of the bonds under consideration.

Synchronicity and concertedness are fundamental mechanistic concepts and give an idea of chemical reactivity. These are used to define the nature of the reaction mechanism of a given process and to establish temporal relationships between the processes of formation/breaking of chemical bonds along the reaction path [38,39]. The absolute synchronicity (Sy) characterizes the chemical reaction in terms of the occurrence of simultaneous chemical processes. It is obtained according to the following expression:

$$S_y = 1 - \left[\frac{1}{(2n-2)}\sum\frac{|\delta\beta_i - \delta\beta_{av}|}{\delta\beta_{av}}\right] \quad (4)$$

If the processes of bond formation/breaking of chemical bonds and/or electron transfer occur simultaneously, then the mechanism is defined as synchronous and concerted, but if they occur at different times (one after the other), the mechanism will be asynchronous [38,39]. Geometric parameters such as symmetry in the distances of bonds that form or break in a transition state (TS) are usually used to determine the synchronicity and concertation of an elementary step [38]. Ideally, a value of zero for this indicator implies total asynchronicity in the reaction, whereas a value of 1 indicates complete synchronicity.

3. Results and discussion

3.1. Reaction mechanisms

The study of the thermal decomposition reaction of benzoylformic acid was undertaken through the examination of three different reaction mechanisms. These mechanisms encompass the decarboxylation and decarbonylation reactions, which account for the primary products acquired in the experimental thermolysis of the molecule under study. The decarboxylation reaction of α-keto acid compounds has been proposed in the literature by two different reaction channels.

Direct decarboxylation was modeled by a four-membered cyclic transition state, involving the migration of a hydrogen atom from the hydroxyl group of the acid to the α-carbonyl, to produce benzaldehyde and carbon dioxide. In the decarbonylation reaction, a molecule of carbon monoxide is released, and a molecule of benzoic acid is obtained. The reaction was modeled through a three-membered cyclic transition state. Fig. 1 represents the proposed reaction channels for the one-step decarbonylation and decarboxylation.

The decarboxylation process of benzoylformic acid has also been modeled by a two-stage mechanism, in the first stage the release of carbon dioxide occurs and the formation of a carbene intermediate, hydroxyphenylcarbene, which in a subsequent stage regroups hydrogen 4 to produce benzaldehyde, as shown in Fig. 2.

Figs. 3 and 4 show the optimized molecular structures of the reactants and products of each reaction studied according to mechanisms 1 and 2.

Fig. 5 shows the optimized structures obtained in the study of the thermal decomposition reaction according to the reaction channel 3. There TS1-3 and TS2-3 represent the transition states in the first and second stage respectively, the intermediate hydroxyphenylcarbene isomerizes to benzaldehyde.

3.2. Preliminary calculations

The thermal decomposition of benzoylformic acid in the gas phase (g) and aqueous solution (aq) was computationally investigated along the previously mentioned reaction pathways and at five different temperatures.

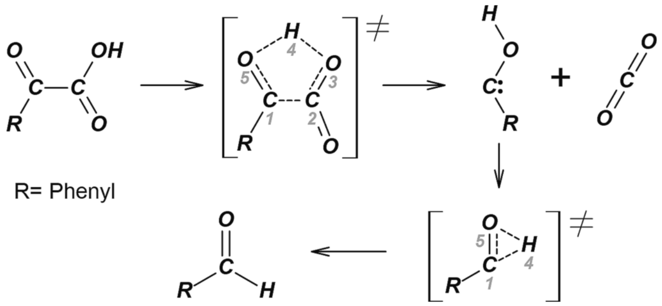

Fig 2. Reaction mechanism for the two-step decarboxylation of benzoylformic acid (reaction channel 3).

To use a suitable method that describes well the system under study, preliminary computational calculations were conducted with Moller Pleset perturbation theory (MP2) and with different density functionals in combination with a 6–311+G(d,p) basis set. Table 1 shows the results of the activation energy (*Ea*) for the one-step decarboxylation of benzoylformic acid (channel 1) using a four-membered cyclic transition state.

According to the obtained results shown in Table 1, the *Ea* for the decarboxylation of benzoylformic acid following channel 1 of the reaction is approximately 20 kcal.mol^{-1} above the experimental value, this occurs with all the functionals used and the closest value is the *Ea* obtained with the PBE functional with a deviation of 47.9%.

Due to the wide difference in *Ea* obtained computationally for the channel 1 with the experimental value, we proceeded to model the decarboxylation reaction through the two-step mechanism (channel 3) using the functional PBE that allowed obtaining values closer to the experimental one according to the Table 1, reaction was also modeled with the most robust PBE0 [40] functional. The modeling was also extended on the thermal decomposition of pyruvic and oxalic acids to amplify the source of comparison.

Table 2 shows results obtained for *Ea*, together with the values reported experimentally. For the oxalic acid reaction there is good agreement between both experimental and computational results with a deviation below 10%. For the pyruvic acid; Taylor, 1987 [41] reports a value of 41.25 kcal.mol^{-1} for thermal decomposition. The author questions the value of 27.7 kcal.mol^{-1} reported by Yamamoto, 1985 [11], while the *Ea* calculated for the reaction is above the experimental value and there is not much difference between the values obtained with the PBE and PBE0 functionals.

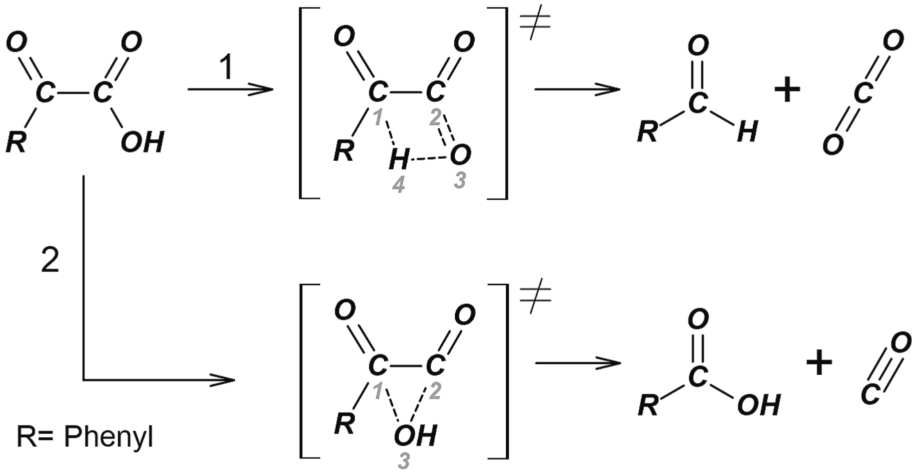

Fig 1. Reaction mechanism studied for the direct decarboxylation (reaction channel 1) and thermal decarbonylation (reaction channel 2) of benzoylformic acid.

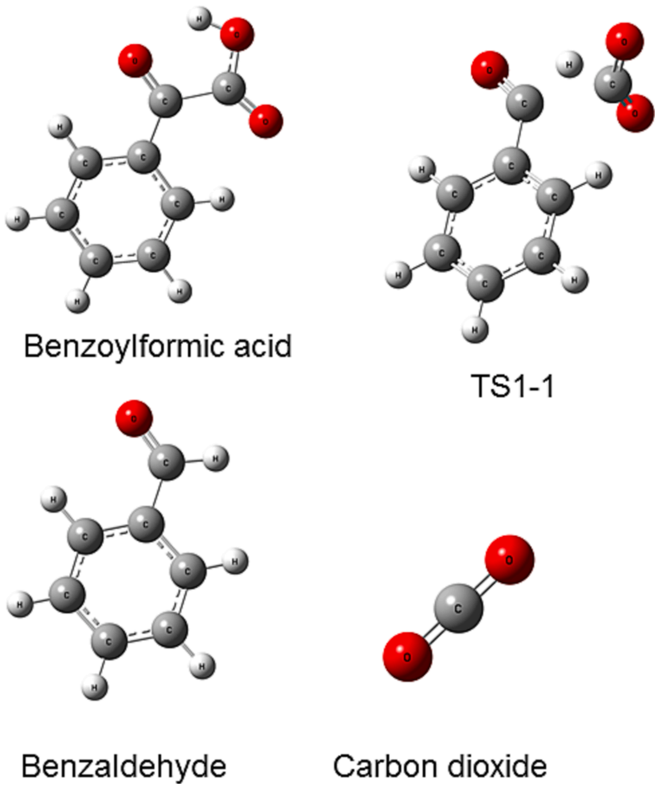

Fig 3. Molecular structures optimized to PBE/6–311+G(d,p) for the reactant, transition state (TS1-1) and products involved in the direct decarboxylation reaction of benzoylformic acid, according to reaction channel 1.

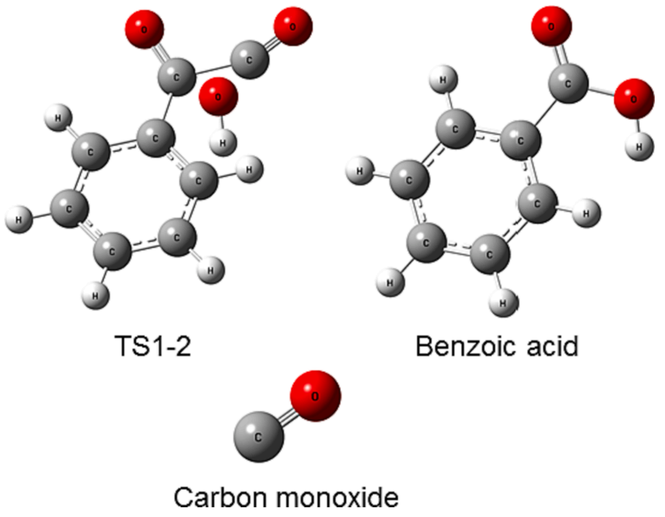

Fig 4. Optimized molecular structures at PBE/6–311+G(d,p) of the TS1-2 transition state and products involved in the decarbonylation reaction of benzoylformic acid according to the reaction channel 2.

Ea obtained at PBE/6–311+G(d,p) for benzoylformic acid differs by approximately 7.8 kcal.mol^{-1}, a 19% of difference from the experimental value. Employing the PBE0 functional does not lead to an enhancement in these findings. Consequently, the computational investigation of the three proposed mechanisms for the thermal decomposition of benzoylformic acid was continued with the PBE functional.

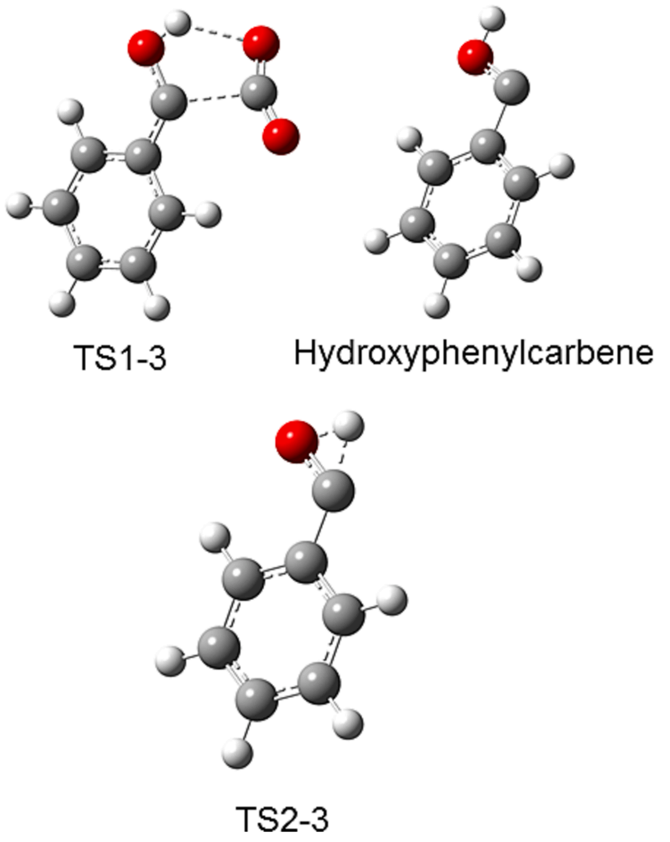

Fig 5. Optimized molecular structures at PBE/6–311+G(d,p) of the transition states TS1-3 and TS2-3 for the first and second reaction steps respectively and the intermediate hydroxyphenylcarbene in the decarboxylation of benzoylformic acid (according to reaction channel 3).

Table 1
Activation energy (*Ea*) for the thermal decarboxylation reaction of benzoylformic acid by the one-step mechanism (reaction channel 1) as a function of different computational calculation methods.

Method	*Ea* (kcal.mol^{-1})
M06-2X	73.3
PBE	60.8
B3LYP	69.9
MP2	68.3
Experimental value [12]	41.1

Table 2
Experimental and computational activation energy (*Ea*) for the decarboxylation of pyruvic, oxalic and benzoylformic acids by the two-step mechanism (reaction channel 3) using PBE and PBE0 functionals and 6–311+G(d,p) basis set. PBE0 calculations are presented in parentheses.

Compound	Computational *Ea* (kcal.mol^{-1}) PBE (PBE0)	Experimental *Ea* (kcal.mol^{-1})	Deviation (%)
Pyruvic acid	61.8 (62.2)	27.7 [11]	123.1 (124.5)
		41.25 [41]	49.8 (50.8)
Oxalic acid	28.3 (31.4)	30 [42]	5.7 (4.7)
		31.2 [43]	9.3 (0.6)
Benzoylformic acid	48.9 (52.3)	41.1 [12]	19.0 (27.3)

3.3. Kinetics and thermodynamics of reactions

Computational calculations of optimization and vibrational frequencies at PBE/6–311+G(d,p) allowed obtaining the kinetic and thermodynamic data for the three reaction channels studied, the results are gathered in Table 3.

Starting the gas-phase analysis, it can be observed that the decarboxylation of benzoylformic acid via reaction channel 3 is kinetically favored, its energy barrier is 205 $kJ.mol^{-1}$ at the rate limiting stage, compared to activation free energies of 218 and 240 $kJ.mol^{-1}$ for decarbonylation and single-stage decarboxylation, respectively. Although the entropic change for the first transition state in stage 1 of mechanism 3 is unfavorable (-10.4 $J.mol^{-1}K^{-1}$), the enthalpic component predominates in its contribution to the activation free energy.

From the thermodynamic point of view, the net decarboxylation reaction is favorable than the decarbonylation. The decarboxylation generates more stable products (carbon dioxide and benzaldehyde) compared to the decarbonylation reaction in which carbon monoxide and benzoic acid are produced.

The second stage of decarboxylation process (Channel 3) presents an energy barrier 94 $kJ.mol^{-1}$, lower than the first stage. The process of hydrogen migration towards carbon 1 (C1) (See Fig. 2) to produce benzaldehyde, occurs rapidly because the carbene intermediate is very thermodynamically unstable ($\Delta G^{g} = 89.1$ $kJ.mol^{-1}$) compared to benzoylformic acid. Fig. 6 shows the reaction profiles as a function of Gibbs free energy for the three reaction channels studied in the gas phase.

When the reaction is analyzed in an aqueous solution, the effect of the solvent allows a decrease in the energy barriers for the all-reaction channels studied. The most important decrease is given for reaction channel 2, which decreases 20.6 $kJ.mol^{-1}$ compared to the decrease of 10.8 and 1.3 $kJ.mol^{-1}$ for channels 1 and 3 in their order.

Observing the geometry of the transition states involved in the three reaction channels in the aqueous phase it is evident in TS1-2 (See Fig. 1) that the hydroxyl group that is transferred from C2 to C1 is quite detached from the rest of the molecule. C1 is situated at 1.97 Å from C2 and 1.73 Å from C1. This arrangement imparts a higher degree of ionic character to the molecule. Consequently, it is possible that this molecular configuration could experience enhanced stabilization through solvation within an aqueous medium. In TS1-1 (See Fig. 1) the hydrogen that is transferred presents bond distances O3-H4 and C1-H4 of 1.3 and 1.5 Å respectively, so the geometry is a little more compact and it is speculated to interact to a lesser degree with the water molecules. TS1-3 is quite advanced, with two well-defined molecular regions giving rise to the intermediate and the carbon dioxide molecule, which decreases the electronic imbalance in the atoms. The activation and reaction free energy for the second stage of decarboxylation (Channel 3) are higher in an aqueous solution because the solvent stabilizes the carbene intermediate to a greater extent by its nature than the stabilization that can occur on TS2 and benzaldehyde.

The reactions were simulated at five different temperatures: 542.7, 553.3, 563.5, 573.3 and 583.6 according to the values used in experiments performed by Taylor [12]. For each temperature, the kinetic constant was calculated using the transition state theory. The linearization of the Arrhenius equation, $lnk = lnA - Ea/RT$, allowed finding the parameters, frequency factor (A) and activation energy (Ea). The values obtained along with the experimental reference parameters are reported in Table 4.

Table 3

Free energy of activation ($\Delta G^{\ddagger}$), reaction energy (ΔG) and enthalpy of activation ($\Delta H^{\ddagger}$), in ($kJ.mol^{-1}$), entropy of activation $\Delta S^{\ddagger}$, in $J.mol^{-1}.K^{-1}$ for the thermal decomposition of benzoylformic acid according to the proposed mechanisms. Computationally obtained at PBE/6–311+G(d,p), at 583.6 K in the gas phase (g) and the aqueous solution (aq).

Reaction channel	$\Delta G^{\ddagger,g}$ $\Delta G^{\ddagger,aq}$	$\Delta H^{\ddagger,g}$ $\Delta H^{\ddagger,aq}$	$\Delta S^{\ddagger,g}$ $\Delta S^{\ddagger,aq}$	ΔG^{g} ΔG^{aq}
1	240.9	249.8	15.2	−125.0
	230.1	254.6	42.1	−139.1
2	218.8	222.3	6.1	−36.8
	198.2	218.6	34.8	−26.8
3	205.3	199.2	−10.4	89.1
stage 1	204.0	214.4	17.9	69.5
3	94.0	92.4	−2.7	−214.1
stage 2	103.2	101.8	−2.4	−208.7

The value calculated for Ea in this work has a deviation of 19% above the value reported by Taylor. The value of 1.1×10^{13} s^{-1} found for the frequency factor (A) is characteristic of first-order reactions.

Despite the disparities between the experimental and computational values, the outcomes derived from the two-step decarboxylation mechanism exhibit greater concordance with the reported experimental data, when contrasted with the outcomes from direct decarboxylation. The results strongly implies that the principal mechanism governing the thermal decomposition of benzoylformic acid involves a two-step decarboxylation process, accompanied by the generation of a carbene intermediate. This mechanism is favored over the currently proposed one-step decarboxylation pathway for the thermal decomposition of benzoylformic acid.

3.4. Synchronicity of reaction

In the optimized structures of the molecules participating in the decarboxylation reaction of benzoylformic acid through reaction channels 1 and 3, the Wiberg bond indices [37] and natural atomic charges were computed for the atoms directly implicated in both the bond-forming and bond-breaking processes.

Equations 1–4 were employed to assess the one-step decarboxylation mechanism (Channel 1), resulting in the determination of the evolution percentages for the C1-C2, C2-O3, O3-H4, and C1-H4 bonds, which were found to be 58.18%, 34.35%, 59.86%, and 32.59%, respectively (See Fig. 1). Complete data can be found in the supporting information. These results indicate that the most advanced process corresponds to the rupture of hydrogen 4 from the hydroxyl group; however, the bond formation involving carbon 1 represents the slowest step in the mechanism. The transition state of the studied mechanism can be characterized by the average relative variation value of the bond index ($\delta Bav = 0.46$). In this case, the value of 0.46 suggests that the transition state is not highly advanced and resemble the reactants more than the products. The absolute synchronicity of the reaction was computed to be 0.82, indicating that the reaction exhibits poor synchronicity. This implies an imbalance between the processes of bond formation and bond breaking. On average, the formation process constitutes approximately 33.5% of the reaction, while bond breaking accounts for an average of 59.2% for the molecule. Consequently, this observation suggests a potential deficit in bonds associated with the one-step decarboxylation mechanism.

The results obtained for the two-stage reaction (Channel 3) are shown in Table 5. In general terms, for the first stage of the reaction (the rate-limiting step), there are very advanced processes, for example, in the hydrogen migration 94.0 % progress is quantified for the breaking of oxygen 3 and 89.0 % in the formation of the new bond with oxygen 5. The elongation of the C1-O5 bond is quantified at 94.6 % progress and 65.5 % for the stretching of C2-O3. The least advanced process concerns carbon–carbon bond breaking, with 48.9 %. A value of 0.78 for the average relative variation enables the characterization of the transition state of the first stage as an advanced structure in which the reaction products of that stage are highly represented. The reaction also has a higher synchronicity than the single stage reaction, it is not fully synchronous especially due to a delay in the C1-C2 bond breaking.

The natural atomic charges were calculated for the atoms directly involved in the reaction center for the decarboxylation of benzoylformic acid, according to reaction channel 3. The values are shown in Table 6.

As evident, the carbon 1 atom undergoes a reduction in its positive charge during the reaction prior to the formation of the ultimate product. In the context of benzoylformic acid, its positive charge is 0.429, while in the transition state of the initial stage, it measures 0.363. These findings lend support to the notion that the decarboxylation transition state experiences stabilization through electron-attracting R groups

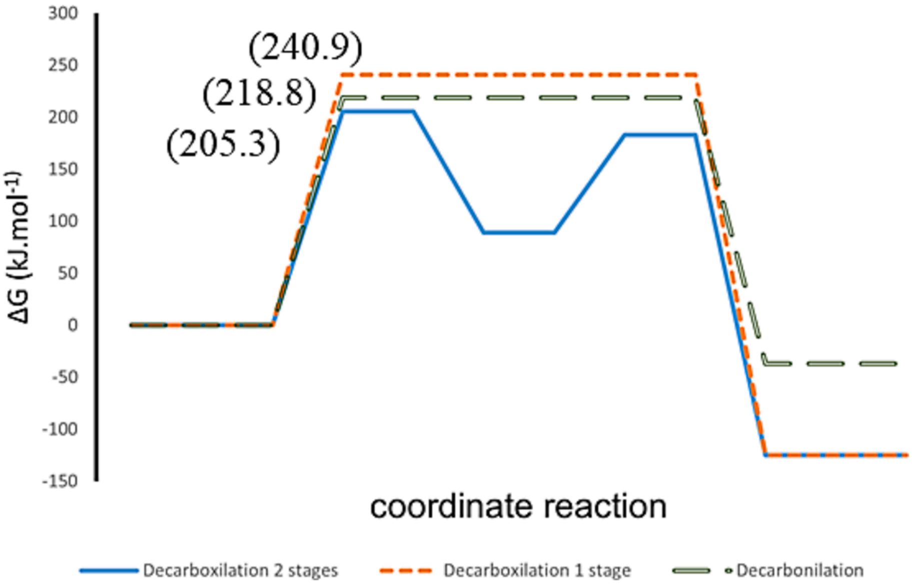

Fig 6. Reaction profile of the thermal decomposition of benzoylformic acid by three different reaction channels, according to Figs. 1 and 2.

situated on the carbon 1 of the molecular framework.

A notable enhancement in charge separation is observed in the atoms constituting the structure of the transition state of stage 1, in comparison with the atomic charges computed for the reactant. The most significant contrast is found within the carbon 1 and carbon 2 atoms. For instance, in the case of benzoylformic acid, the charge difference between C2 and C1 atoms is 0.249. However, this difference expands to 0.455 in the transition state. Evidently, this carbon–carbon bond can be perceived as a demarcation region, delineating two considerably advanced molecular domains.

Table 4
Experimental and calculated Arrhenius parameters at PBE/6–311+G(d,p) according to the two-step mechanism for the gas-phase decarboxylation reaction of benzoylformic acid.

Computational		Experimental [12]	
Ea (kJ.mol^{-1})	ln *A* (s^{-1})	*Ea* (kJ.mol^{-1})	ln *A* (s^{-1})
204.7	30.0	171.9[1]	34.0[2]

[1] conversion of kcal to kJ.
[2] conversion of log A to ln A.

Table 5
Percent evolution (%EV), average relative variation (δB$_{av}$) and absolute synchronicity (S$_y$) for the thermal decomposition reaction of benzoylformic acid using reaction channel 3. Calculated at PBE/6–311+G(d,p) in the gas phase. See atom labeling in Fig. 2.

Stage	**Indicator**	**Bond** **C1-C2**	**C2-03**	**O3-H4**	**O5-H4**	**C1-O5**
1	*%EV*	48.9	65.5	94.0	89.0	94.6
	δB$_{av}$			0.78		
	S_y			0.86		
		C1-H4		O5-H4	C1-O5	
2	*%EV*	47.0		58.3	58.9	
	δB$_{av}$			0.53		
	S_y			0.94		

Table 6
Natural atomic charges were calculated for reactant, transition states (TS1-3 and TS2-3), intermediate and products for the two-step decarboxylation (see Fig. 2).

Species	**Atom**				
	C1	C2	O3	H4	O5
Benzoylformic acid	0.429	0.678	−0.626	0.489	−0.540
TS1	0.363	0.818	−0.620	0.522	−0.616
Carbene	0.168	—	—	0.490	−0.634
TS2	0.118	—	—	0.472	−0.620
Products	0.379	0.921	−0.461	0.113	−0.501

4. Conclusions

The computational analysis of the thermal decomposition reaction of benzoylformic acid was carried out by investigating three distinct reaction channels, which account the principal experimentally obtained products. In reaction channel 1, the decarboxylation of the reactant occurs in a single step, while reaction channel 2 models decarbonylation. The third chemical process under study corresponds to a two-step decarboxylation reaction mechanism. The kinetic and thermodynamic values associated with each studied reaction mechanism provide evidence that supports the plausibility of the two-stage decarboxylation mechanism depicted in Fig. 2 for the thermal decomposition of the studied compound. It is noteworthy that the first stage governs the rate-limiting step.

Results from the simulation involving water as a solvent using the IEFPCM method shows a reduction in the energy barrier and thermodynamic favoring each chemical process. However, in the context of the two-stage decarboxylation mechanism, the solvent effect remains less evident. Given that the transition state (TS1-3) in the initial stage of the reaction exhibits significant advancement, while in the second stage, the carbene intermediate attains greater stabilization relative to TS2-3 and the benzaldehyde, and it explains why the solvent does not reduce the energy barrier.

Calculation of the Wiberg bond indices provided a quantifiable measure of progress in both bond formation and bond cleavage within the decarboxylation reaction. In the two-step decarboxylation mechanism (Channel 3), the formation of the carbene intermediate occurs through a highly advanced transition state (δBav = 0.78). These results indicate a 94% advancement in the migration of hydrogen 4, leading to the detachment of oxygen 3, and an 89% progression in the formation of the new bond with oxygen 5. This mechanism is rate-limited by the first stage and is characterized as a concerted but slightly synchronous reaction.

CRediT authorship contribution statement

Daniel Giraldo: Methodology, Investigation, Writing – original draft, Writing – review & editing. **Daniela Becerra:** Methodology, Investigation. **Silvia Quijano:** Writing – review & editing. **Pablo Ruiz:** Conceptualization, Investigation, Writing – original draft, Writing – review & editing. **Jairo Quijano:** Supervision. **Jair Gaviria:** Supervision.

Declaration of Competing Interest

The authors declare that they have no known competing financial interests or personal relationships that could have appeared to influence the work reported in this paper.

Data availability

Data will be made available on request.

Acknowledgments

The authors are grateful for the support received from the Universidad Nacional de Colombia - Sede Medellín during the research and publication stages of this work. D.G. Thanks to the Minas Faculty from Universidad Nacional de Colombia - Sede Medellín. S.Q. Thanks to the Dirección General de Investigación (DGI) of the Universidad Santiago de Cali, Santiago de Cali. P.R. also thanks the Instituto Tecnológico Metropolitano (ITM), Medellín - Colombia.

Funding Open Acces funding provided by Colombia Consoritum.

Appendix A. Supplementary material

Supplementary data to this article can be found online at https://doi.org/10.1016/j.comptc.2023.114337.

References

[1] Y.C. He, et al., Biosynthesis of benzoylformic acid from benzoyl cyanide by a newly isolated Rhodococcus sp. CCZU10-1 in toluene-water biphasic system, Bioresour. Technol. 115 (2012) 88–95.

[2] A. Malpica, M. Calzadilla, I. Mejias, Kinetics and mechanism for oxime formation in the dehydration electrostatic interactions from benzoylformic acid: of carbinolamines, Int. J. Chem. Kinet. 40 (2008) 554–558.

[3] Z. Zhang, et al., Visible-light-mediated direct access to α-ketoamides by dealkylative amidation of tertiary amines with benzoylformic acids, Tetrahedron Lett. 60 (43) (2019), 151191.

[4] G.S. Koutoulogenis, N. Spiliopoulou, C.G. Kokotos, Photochemical C-H acetalization of O-heterocycles utilizing phenylglyoxylic acid as the photoinitiator, Photochem. Photobiol. Sci. 21 (5) (2022) 687–694.

[5] W. Lunkenheimer, A. Wittig, W. Draber, T. H., “Process for the preparatoin of phenylglyoxylic acid esters,” 4596885, 1986.

[6] I. Nongkynrih, M.K. Mahanti, Quinolinium dichromate oxidations. Kinetics and mechanism of the oxidative cleavage of styrenes, J. Org. Chem. 58 (18) (1993) 4925–4928.

[7] L. Feldberg, Y. Sasson, Copper-catalysed oxidation of hydroxy compounds by tert-butyl hydroperoxide under phase-transfer conditions, J. Chem. Soc. Chem. Commun. no. 15 (1994) 1807.

[8] Y.C. He, J.H. Xu, J. Pan, L.M. Ouyang, Y. Xu, Preparation of (R)-(-)-mandelic acid and its derivatives from racemates by enantioselective degradation with a newly isolated bacterial strain Alcaligenes sp. ECU0401, Bioprocess Biosys. Eng. 31 (2008) 445–451.

[9] A.J.L. Cooper, J.Z. Ginos, A. Meister, Synthesis and properties of the α -keto acids, Chem. Rev. 83 (1983) 321–358.

[10] C.D. Hurd, H.R. Raterink, The Decomposition of Alpha Keto Acids, J. Am. Chem. Soc. 56 (6) (1934) 1348–1350.

[11] S. Yamamoto, R.A. Back, The photolysis and thermal decomposition of pyruvic acid in the gas phase, Can. J. Chem. 63 (2) (1985) 549–554.

[12] R. Taylor, The mechanism of thermal eliminations. Part XXVIII [1]: Thermal decomposition of benzoylformic acid, Int. J. Chem. Kinet. 23 (3) (1991) 247–250.

[13] K. Saito, G. Sasaki, K. Okada, S. Tanaka, Unimolecular decomposition of pyruvic acid: An experimental and theoretical study, J. Phys. Chem. 98 (14) (1994) 3756–3761.

[14] P. Leermakers, G. Vesley, The Photochemistry of a-Keto Acids and a-Keto Esters, J. Am. Chem. Soc. 85 (23) (1963) 3776–3779.

[15] X. He, W. Jia, Y. Gao, S. Jiang, J. Nie, F. Sun, Water-soluble benzoylformic acid photoinitiators for water-based LED-triggered deep-layer photopolymerization, Eur. Polym. J. vol. 167, no. February (2022), 111066.

[16] R.A. Back, S. Yamamoto, The gas-phase photochemistry and thermal decomposition of glyoxylic acid, Can. J. Chem. 63 (2) (1985) 542–548.

[17] L. Chen, G. Chen, X. Fu, Theoretical studies on the mechanism of the thermal decarboxylation and decarbonylation of a number of α-keto-acids, Chinese J. Chem. 13 (6) (1995) 487–492.

[18] J. Higgins, X. Zhou, R. Liu, T.T.S. Huang, Theoretical study of thermal decomposition mechanism of oxalic acid, Chem. A Eur. J. 101 (14) (1997) 2702–2708.

[19] M. Khavani, M. Izadyar, A. Jamsaz, DFT investigation of the kinetics and mechanism of the thermal decomposition of oxalic acid, Prog. React. Kinet. Mech. 42 (1) (2017) 44–51.

[20] M.D.P. Barquilla, M.L. Mayes, A computational study of the gas-phase pyruvic acid decomposition: Potential energy surfaces, temporal dependence, and rates, AIP Adv. 11 (1) (2021) 1–8.

[21] F.D. Frisch MJ, Trucks GW, Schlegel HB, Scuseria GE, Robb MA, Cheeseman JR, Scalmani G, Barone V, Mennucci B, Petersson GA, Nakatsuji H, Caricato M, Li X, Hratchian HP, Izmaylov AF, Bloino J, Zheng G, Sonnenberg JL, Hada M, Ehara M, Toyota K, Fukuda R, Hasegaw, “Gaussian 09, Revision B.01.” Gaussian, Inc., Wallingford CT, 2010.

[22] Y. Zhao, D.G. Truhlar, The M06 suite of density functionals for main group thermochemistry, thermochemical kinetics, noncovalent interactions, excited states, and transition elements: Two new functionals and systematic testing of four M06-class functionals and 12 other function, Theor. Chem. Acc. 120 (1–3) (2008) 215–241.

[23] J.P. Perdew, K. Burke, M. Ernzerhof, Generalized gradient approximation made simple, Phys. Rev. Lett. 77 (18) (1996) 3865–3868.

[24] A. Becke, Density-functional thermochemistry. III. The role of exact exchange, J. Chem. Phys. 98 (7) (1993) 5648–5652.

[25] C. Møller, M. Plesset, Note on an approximation treatment for many-electron systems, Phys. Rev. 46 (1934) 618–622.

[26] R. Ditchfield, W. Hehre, J. Pople, Self-Consistent Molecular-Orbital Methods. IX. An Extended Gaussian-Type Basis for Molecular-Orbital Studies of Organic Molecules, J. Chem. Phys. 54 (2) (1971) 724–728.

[27] D. Rappoport, N. R. M. Crawford, F. Furche, and K. Burke, “Which functional should I choose?,” Comput. Inorganicand Bioinorg. Chem., vol. 594, 2008.

[28] D.A. McQuarrie, J.D. Simon, Molecular Thermodynamics, University Science Books, Sausalito, 1999.

[29] J. Tomasi, B. Mennucci, R. Cammi, Quantum mechanical continuum solvation models, Chem. Rev. (2005).

[30] A. Klamt, C. Moya, J. Palomar, A Comprehensive Comparison of the IEFPCM and SS(V)PE Continuum Solvation Methods with the COSMO Approach, Chem. Theory Comput. 11 (9) (2015) 4220–4225.

[31] K. Fukui, A Formulation of the Reaction Coordinate, J. af Phys. Chem. 74 (23) (1970) 4161–4163.

[32] K.J. Glasstone, K.J. Laidler, H. Eyring, The Theory of Rate Processes, McGraw-Hill, New York, 1941.

[33] S.W. Benson, The Foundations of Chemical Kinetics, McGraw-Hill, New York, 1969.

[34] A.E. Reed, F. Weinhold, Natural bond orbital analysis of near-Hartree–Fock water dimer, J. Chem. Phys. 78 (6) (Mar. 1983) 4066–4073.

[35] A.E. Reed, L. a. Curtiss, and F. Weinhold, Intermolecular interactions from a natural bond orbital, donor-acceptor viewpoint, Chem. Rev., Sep. 88 (6) (1988) 899–926.

[36] E.D. Glendening, A.E. Reed, J.E. Carpenter, F. Weinhold, NBO, Madison, WI, 1988.

[37] K.B. Wiberg, Application of the pople-santry-segal CNDO method to the cyclopropylcarbinyl and cyclobutyl cation and to bicyclobutane, Tetrahedron 24 (3) (1968) 1083–1096.

[38] M.A.F. De Souza, E. Ventura, S.A. Do Monte, J.M. Riveros, R.L. Longo, Revisiting the concept of the (a)synchronicity of diels-alder reactions based on the dynamics of quasiclassical trajectories, J. Comput. Chem. 37 (8) (2016) 701–711.

[39] A.I. Adjieufack, et al., How effectively bonding evolution theory retrieves and visualizes curly arrows: The cycloaddition reaction of cyclic nitrones, Int. J. Quantum Chem 119 (19) (2019) 1–14.

[40] C. Adamo, V. Barone, Toward reliable density functional method without adjustable parameters: The PBE0 model, J. Chem. Phys. 110 (1999) 6158–6170.

[41] R. Taylor, The mechanism of thermal eliminations part XXIII: [1] The thermal decomposition of pyruvic acid, Int. J. Chem. Kinetic 19 (8) (1987) 709–713.

[42] G. Lapidus, D. Barton, P. Yankwich, Kinetics and stoichiometry of the gas-phase decomposition of oxalic acid, J. Phys. Chem. 68 (7) (1964) 1863–1865.

[43] T. Kakumoto, K. Saito, A. Imamura, Unimolecular decomposition of oxalic acid, J. Phys. Chem. 91 (9) (1987) 2366–2371.